J Electroceram (2011) 27:51–55
DOI 10.1007/s10832-011-9649-4

Investigations of lanthanum doping on magnetic properties of nano cobalt ferrites

Pawan Kumar · S. K. Sharma · M. Knobel · Jagdish Chand · M. Singh

Received: 17 February 2010 / Accepted: 11 July 2011 / Published online: 26 July 2011

Abstract The magnetic properties of nano-crystallite cobalt lanthanum ferrite ($CoLa_xFe_{2-x}O_4$) with varied quantities of lanthanum (x=0, 0.1, 0.15, 0.2, 0.25, 0.3) prepared by co-precipitation method have been studied by vibrating sample magnetometer (VSM) and LCR meter. X-ray diffraction (XRD) and transmission electron microscopy (TEM) confirmed the size, structure, and morphology of the ferrite samples. The average crystallite size varied from 17.83 nm to 49.99 nm. All the samples, although, in nano range, show significant hysteresis. The saturation magnetization (M_s) values decreased from 60.57 emu/g to 30.15 emu/g. The remanence (M_R) fell from 10.85 emu/g to 6.39 emu/g. Doping with lanthanum La^{3+} ions modulates significantly the magnetic properties of cobalt spinel ferrites without sacrificing the ferromagnetic character.

Keywords Coprecipitation · Saturation magnetisation · Permeability · Ferrite

1 Introduction

Nanoscale materials possess intriguing properties that are comparable to or superior to those of bulk. These materials are interesting due to their fascinating size dependent optical, electronic, magnetic, thermal, mechanical and chemical properties [1]. Cobalt ferrites have been regarded as one of the competitive candidates for high density magnetic recording media because of its moderate saturation magnetization, high coercivity, mechanical hardness and chemical stability [2]. Synthesis of nanoparticles, especially spinel ferrites, characterized by a small size distribution is important. Small particle size of the prepared particles offers large contact area for solid state reaction during sintering process. In addition to this, other benefits of small size are shorter diffusion routes, elimination of porosity and compaction is also better. Another advantage is that grain growth can also be controlled [3]. Spinel ferrites have remarkable electrical and magnetic properties and wide practical applications in information storage systems, ferro-fluid technology, magneto-caloric refrigeration and magnetic diagnostics[4]. For all the magnetic nanoparticles there is a critical size dimension (D_{sp}) below which it will be superparamagnetic with no hysteresis and no remanence. So the useful particle size should be in the range $D_{sp}<D<D_{sd}$ where D_{sd} is single domain size [5].

Our interest is to make cobalt ferrites at nano scale with magnetic properties similar to bulk material and then to modulate the properties by doping with La^{3+} ions.

2 Experimental details

La-Co ferrite of composition $CoLa_xFe_{2-x}O_4$ (x=0, 0.1, 0.15, 0.2, 0.25, 0.3) was prepared by the co-precipitation method [6, 7]. The materials used were cobalt nitrate (97% Merck, India), iron nitrate (98% Merck, India), lanthanum nitrate (Merck, Germany) and sodium hydroxide (96% Merck, India). Sodium hydroxide (27 g) was dissolved in 2 L of distilled water to have the concentration of 0.33 mol/L and heated to boiling. The pH of the solution lies in the range

P. Kumar (✉) · J. Chand · M. Singh
Department of Physics, Himachal Pradesh University, Shimla, India
e-mail: pawankumarsolan@gmail.com

S. K. Sharma · M. Knobel
Instituto de Fisica Gleb Wataghin, Universidade Estadual de Campinas (UNICAMP), Campinas 13.083-970 SP, Brazil

13–14. Cobalt nitrate, lanthanum nitrate and iron (III) nitrate were taken in accurate stoichiometric proportions and dissolved and then added to sodium hydroxide solution already prepared. The solution was poured as quickly as possible into the boiling solution of NaOH under vigorous stirring produced by the glass mechanical stirrer (500 rpm). Mixing is very important; otherwise segregation of phases can take place. Precipitates were washed with distilled water (900 ml) and centrifuged at 7000 rpm for 10 min. The residue was dried and powdered. These samples were sintered in air at 500°C at a heating rate of 350°C/h for 3 h and were subsequently cooled. This powder was mixed with 2% P.V. A. binder and pressed into pellets and rings uniaxially under a pressure of 5 ton/inch^2 in a stainless steel die. These samples were then sintered in air at 500°C for 3 h and were subsequently cooled. The rings were wound with about 42 turns of 34 SWG enameled copper wire to form the toroids. Saturation magnetization and magnetic remanence were measured by using vibrating sample magnetometer (VSM). XRD was taken with XPERT-PRO system. Permeability studies were done with LCR meter from Agilent Technologies 4285A. The dc resistivity of the sample at different temperatures was measured by using a Keithley-2611 system.

3 Result and discussion

The X-ray diffraction patterns for the ferrite powder obtained on calcination at 500°C shows a typical single-phase inverse spinel structure and are shown in Fig. 1. The diffraction peaks are broad because of the nanometer size of the crystallite. The particle size of the samples has been estimated from the broadening of XRD peaks using the Scherrer equation [8]. It has been found to lie between 17 nm and 49 nm (Table 1). The particle size is also supported by TEM (Fig. 2).

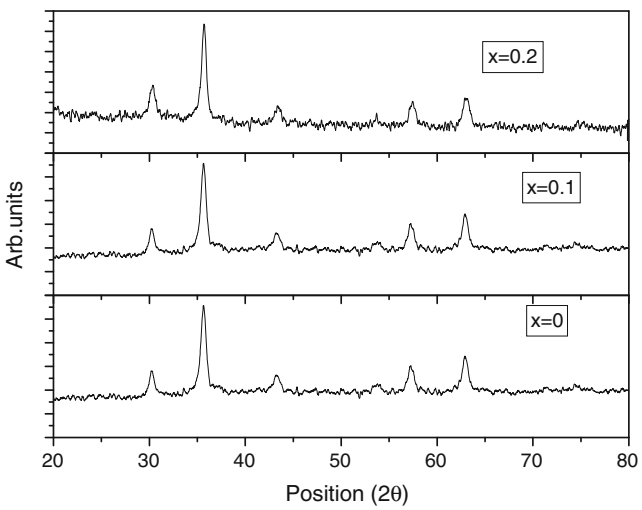

Fig. 1 XRD of $CoLa_xFe_{1-x}O_4$ for x=0.0, 0.1, 0.2

Cobalt ferrites are studied in literature extensibly. For example, B.G. Toksha et al. [9] prepared 11–40 nm cobalt ferrite particles by sol–gel method. The saturation magnetization for pure cobalt ferrites is comparable to our values (Table 1, Fig. 3) while remanence and coercivity are higher. When some Fe^{3+} ions are substituted by La^{3+} ions, the lattice parameters are changed. The lattice parameters may increase or decrease depending upon the result of two effects. The large size of La^{3+} tries to increase the lattice parameter and the strain produced by its substitution in the cell, tries to decrease it. This has been investigated by many researchers [10, 11].

If the sample prepared grows into a pure inverse type spinel structure with all Co^{2+} ions located in the octahedral sub lattice, the magnetization per formula unit is represented by the net moment of that in A and B sites. A simple theoretical expression for the net moments of $CoLa_{0.1}Fe_{1.9}O_4$ can be written as (assuming La^{3+} ions are only in the B sites, for their large ion radii) : $M_{La} = M_B - M_A = [5 \times 0.9 + 3.8 + 0.1 \times \mu_{La}] - 5 = 3.3 + 0.1 \times 0 = 3.3\ \mu_B$ where M_A and M_B represent the total magnetic moment of the A and B sub lattices, respectively. The magnetic moment of Fe^{3+} cations is fixed to be 5 μ_B (spin only) and that of octahedrally coordinated Co^{2+} cations is fixed to be 3.8 μ_B which corresponds to the saturation magnetization at 0 K of bulk $CoFe_2O_4$ (95emug^{-1}) [12]. The net magnetic moment for La^{3+} has been taken to be zero, La^{3+} being non-magnetic. So the saturation magnetization is expected to be less than pure $CoFe_2O_4$ (x=0). The measurements (Figs. 4, 5) show that saturation magnetization decreases with the increase of La^{3+} ions. This can be related to the decrease in Fe^{3+}–Fe^{3+} (B–B) interactions resulting from doping with La^{3+} ions. The La^{3+}–Fe^{3+} interaction as well as the La^{3+}–La^{3+} may exist but they are very weak [11, 13]. However, the M_S does not decrease linearly with La^{3+} concentration. This can be attributed to variation in size and surface effects in nano materials [14–16]. For the same reasons the decrease of M_R with concentration (x) of La^{3+} (Table 1) can be understood. Figure 5 also shows that although all the samples are in nano-range but still show appreciable hysteresis with good value of saturation magnetization and remanence at room temperature also. However, H_C does not follow the variation of M_S and M_R. Its variation depends upon a number of factors like microstructure, particle/grain size, residual strain and many other complex factors [17–19].

It has been found that ultrafine particles of magnetic materials are superparamagnetic below a certain critical size and finite temperature [14]. This is applicable for particles with size below 25 nm. Although most of the compositions (except x=0.1) are above this value but it is possible in all

Table 1 Particle size, remanence (M_R), saturation magnetization (M_S) and coercivity (H_C) at different La^{3+} ions concentration

Composition ($CoLa_xFe_{1-x}O_4$)	Particle size (nm)	M_R (emu/g)	M_S (emu/g)	H_C (Oe)
x=0.00	49.84	10.85	60.57	215.45
x=0.10	17.83	7.70	47.13	153.32
x=0.15	49.97	7.55	42.34	172.87
x=0.20	27.73	7.38	40.31	168.98
x=0.25	38.45	7.002	36.89	194.02
x=0.30	20.78	6.39	30.15	209.76

other composition as well that there may be particle size distribution although average is above this value. This may be probably the case that is why the pure $CoFe_2O_4$ has lower saturation magnetization in comparison to bulk value. The other causes of this reduction can be change in magnetic structures on the surface and canted spin structures on surface.

In general, the initial permeability (μ_i) of spinel ferrites is related with saturation magnetization (M_S) and magnetic anisotropy as $\mu_i \propto M_S{}^n/|K|^{n/2}$, where K is the magnetic anisotropy and M_S is the saturation magnetization [20]. Here n=1 for domain wall displacement and n=2 for magnetization rotation. As μ_i is proportional to $M_S{}^2$, the variation of μ_i with x for La^{3+} should be affected in a manner similar to that of variation of $M_S{}^2$ with x. From this graph (Fig. 6) it is inferred that the variation of μ_i with La^{3+} ion concentration shows a large change than produced by $M_S{}^2$ alone. This means that in addition to the variation of M_S, the magnetic anisotropy K does play a significant role in affecting the value of initial permeability, with an increase in the La^{3+} ion concentration. Qualitatively, the variation of K can be explained on the basis of single ion anisotropy model [21], which shows that the Fe^{3+} ions at the tetrahedral site are compensated by the negative anisotropy of Fe^{3+} ions at the octahedral site. As the concentration of the La^{3+} is increased, the cation distribution of Fe^{3+} ions is modified. This results in a different number of Fe^{3+} ions present at both sites, which in turn affects K. Although Fe^{2+} ions are inevitably formed during the sintering process, yet they are not contributing significantly to the anisotropy energy in our samples.

The initial permeability, μ_i, as a function of the concentration x for La^{3+} ions is shown in Fig. 6. This curve (Fig. 6) shows that at first μ_i decreases to a minimum at x=0.10, and then increases non-linearly with the concentration of La^{3+}. The variation of μ_i with concentration of La^{3+} is not affected in a manner similar to the variation of $M_S{}^2$ with concentration of La^{3+}. In this case the magnetic anisotropy plays an important role in the variation of μ_i with the concentration of La^{+3}. The anisotropy field first increases with the addition of La^{3+} ions and then decreases (Fig. 7). These variations are also reflected in the variations of μ_i with of La^{3+} concentration (Fig. 6).

Magnetic anisotropy (K) is largely contributed by Magneto-crystalline anisotropy K_1 and $K_1 = c\ M_S\ H_a$ [20] can be determined from permeability versus frequency using $H_a=2\pi f_r/\nu$, where f_r is resonance frequency in μ_i vs frequency curve and ν is the gyromagnetic constant given by $\nu=8.791\times10^6$ g (Oe^{-1} s^{-1}), where g is gyromagnetic ratio. The anisotropy field thus calculated with the

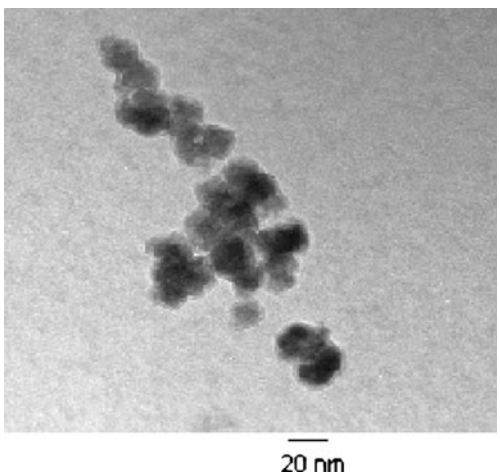

Fig. 2 TEM of $CoLa_xFe_{1-x}O_4$ for x=0.3

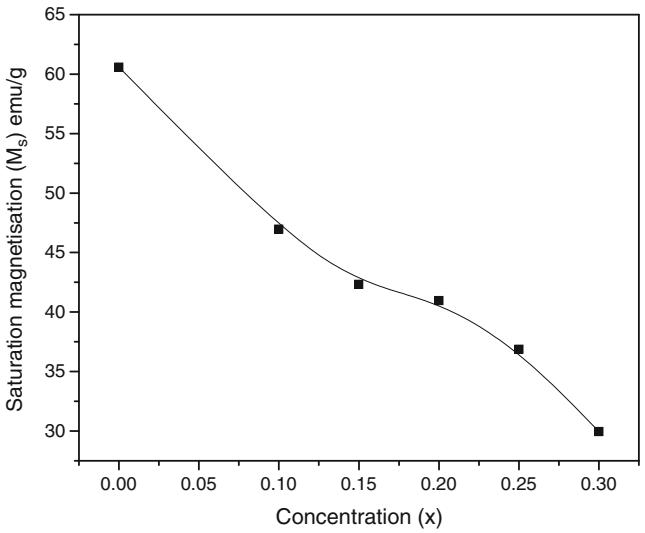

Fig. 3 Variation of saturation magnetization (M_S) as a function of La^{3+} ions concentration

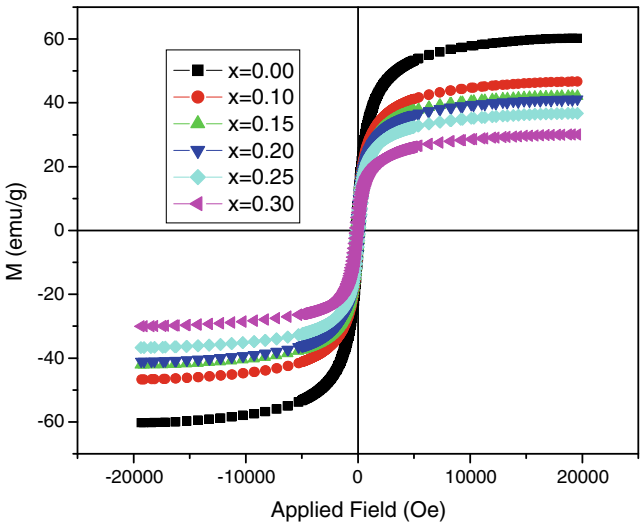

Fig. 4 Hysteresis curves for $CoLa_xFe_{1-x}O_4$ for x=0, 0.1, 0.15, 0.2, 0.25, 0.3 at 300 K

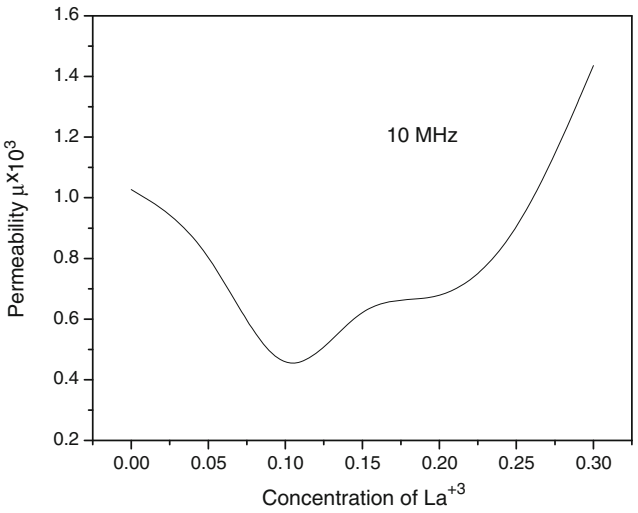

Fig. 6 Variation of permeability (μ_i) as a function of La^{3+} ions concentration

assumption of g=2 as a function of La^{+3} ion concentration is shown in Fig. 7.

Now the variation of permeability with concentration can be understood, at least qualitatively, using the variation of magnetic saturation (Fig. 3) and anisotropic field (Fig. 7) with concentration.

4 Conclusions

The nano particles of cobalt lanthanum ferrite ($CoLa_xFe_{2-x}O_4$) with varied quantities of lanthanum (x=0, 0.1, 0.15, 0.2, 0.25, 0.3) were prepared by co-precipitation method. Particles size lies in the range of 17 nm to 49 nm. The particle size is measured by Scherrer equation from XRD and TEM and are in very good agreement with each other indicating that there was no agglomeration and that the size distribution of the prepared nanoparticles is small. All the samples, although, in nano range show significant hysteresis. We have successfully modulated the properties of cobalt ferrite without losing the ferromagnetic character. The structure is found to be spinel. Saturation magnetization decreases from 60.57 emu/g to 30.15 emu/g. The decrease in saturation magnetization with the increase of La^{3+} ions can be related to the decrease in Fe^{3+}–Fe^{3+} (B–B) interactions resulting from doping with La^{3+} ions. The La^{3+}–Fe^{3+} interaction as well as the La^{3+}–La^{3+} may exist but they are very weak. Variation of saturation magnetization and permeability is explained on the basis of variation of anisotropic field. Variation of coercivity (H_C) does not follow any particular trend and this has been attributed to its

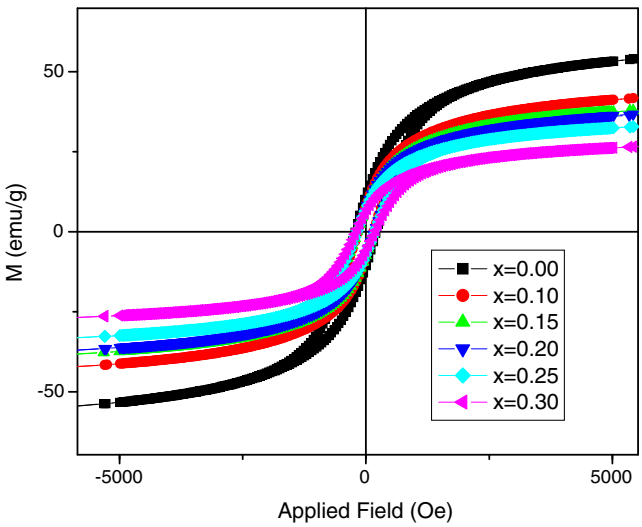

Fig. 5 Magnified view of hysteresis curves for $CoLa_xFe_{1-x}O_4$ for x=0, 0.1, 0.15, 0.2, 0.25, 0.3 at 300 K

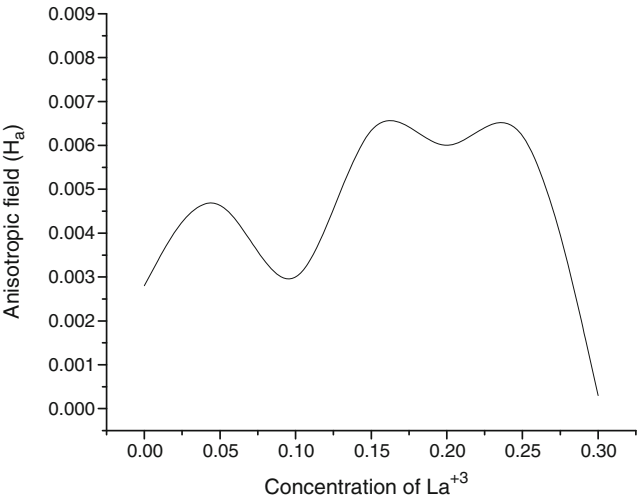

Fig. 7 Anisotropic field H_a versus La^{+3} concentration

dependence upon a plethora of factors like microstructure, particle/grain size, residual strain and many other complex factors.

References

1. S. Thakur, S.C. Katyal, M. Singh, J. Magn. Magn. Mater. **1**, 321 (2009)
2. S. Singhal, S.K. Barthwal, K. Chandra, J. Magn. Magn. Mater. **306**, 233 (2006)
3. R. Valenzuela, *Magnetic Ceramics*. (Cambridge University Press, New York, 1994)
4. M.J. Iqbal, M.R. Siddiquah, J. Alloys.Compd. **453**, 513 (2008)
5. C. Yan, F. Cheng, Z. Peng, Z. Xu, C. Liao, J. Appl. Phys. **84**, 5703 (1998)
6. P. Mathur, A. Thakur, M. Singh, Mod. Phys. Lett. B **21**, 1425 (2007)
7. P. Kumar, S.K. Sharma, M. Knobel, M. Singh, J. Alloys Compd. **508**, 115 (2010)
8. B.D. Cullity, *Elements of x-ray diffraction* (Addison-Wesley, Reading, 1978)
9. B.G. Toksha, S.E. Shirsath, S.M. Patange, K.M. Jadhav, Solid State Comm. **147**, 479 (2008)
10. L. Zhao, H. Yang, L. Yu, Yuming, X. Zhao, S. Feng, J. Mater. Sci. **42**, 686 (2007)
11. L. Ben Tahar, M. Artus, S. Ammar, L.S. Smiri, F. Herbst, M.J. Vaulay, V. Richard, M. Greneche, F. Villain, F. Fievet, J. Magn. Magn. Mater. **320**, 3242 (2008)
12. M.L. Kahn, Z.J. Zhang, Appl. Phys. Lett. **78**, 3651 (2001)
13. N. Rezlescu, E. Rezlescu, C. Pasnicu, M.L. Craus, J. Phys.: Condens. Matter **6**, 5707 (1994)
14. R.N. Panda, J.C. Shih, T.S. Chin, J. Magn. Magn Mat. **257**, 79 (2003)
15. S. Prasad, N.S. Gajbhiye, J. Alloys Compd. **265**, 87 (1998)
16. A.T. Ngo, P. Bonville, M.P. Pileni, J. Appl. Phys. **89**, 3370 (2001)
17. S.H. Xiao, H.J. Xu, J. Hu, L.Y. Li, X.J. Li, Physica E **40**, 3064 (2008)
18. B.H. Liu, J. Ding, Appl. Phys. Lett. **88**, 042506 (2006)
19. Y.C. Wang, J. Ding, J.B. Yi, B.H. Liu, T. Yu, Z.X. Shen, Appl. Phys. Lett. **84**, 2596 (2004)
20. Sun-Ho Kang, H. Yoo III, J. Appl. Phys **88**, 4754 (2000)
21. R.F. Pearson, A.D. Annis, J. Appl. Phys. **39**, 1338 (1968)